Experimental Bidirectional SAR ATI acquisitions of the ocean surface with TanDEM-X

Paco López-Dekker, German Aerospace Center (DLR), Francisco.LopezDekker@dlr.de, Germany
Marc Rodríguez-Cassola, German Aerospace Center (DLR), Marc.Rodriguez@dlr.de, Germany
Pau Prats, German Aerospace Center (DLR), Pau.Prats@dlr.de, Germany
Francesco De Zan, German Aerospace Center (DLR), Francesco.DeZan@dlr.de, Germany
Thomas Kraus, German Aerospace Center (DLR), T.Kraus@dlr.de, Germany
Stefan Sauer, German Aerospace Center (DLR), Stefan.Sauer@dlr.de, Germany
Josef Mittermayer, German Aerospace Center (DLR), Josef.Mittermayer@dlr.de, Germany

Abstract

This paper discusses observations of the ocean surface using a combination of along-track SAR interferometry and the recently proposed Bidirectional SAR acquisition mode. The paper discusses the expected performance, and shows first experimental results with TanDEM-X acquisitions.

1 Introduction

Since first proposed by Goldstein *et.al.* [1], Along-Track SAR Interferometry (ATI SAR) has been considered by numerous authors as a technique to infer ocean surface velocities. Indeed, by generating a pair of SAR images of a surface under nearly identical geometry and with a short time-lag, the ATI phase provides an estimate of the first moment of the Doppler spectrum associated to the surface motion. It is worth pointing out, however, that the retrieved mean Doppler frequency cannot be directly translated into an ocean current component: it provides a NRCS weighted average of the radial velocities, where the coupling between NRCS and velocity modulations by the underlying wave-field result in strong sea-state dependent biases. This is clearly illustrated by the strong correlation between Doppler centroid anomalies and surface winds in ENVISAT's ASAR observations [2].

Assuming that these geophysical biases can be dealt with, for example by simultaneously resolving the surface wind vector, it is intuitively clear that ATI-SAR observations of the ocean surface can provide valuable information regarding the ocean surface current [3].

In a typical ATI configuration, with a common transmitter and two receive-phase centers separated along-track by a physical distance B_{AT}, the ATI phase ($\Delta\phi_{\mathrm{ATI}}$) is related to the effective (NRCS weighted average) radial velocity (v_r) by:

$$\Delta\phi_{\mathrm{ATI}} = -2\pi\frac{B_{\mathrm{AT}}}{\lambda}\cdot\frac{v_r}{v_{\mathrm{orb}}}, \tag{1}$$

where λ is the radar wavelength, v_{orb} the platform velocity, and where

$$\tau_{\mathrm{ATI}} = \frac{B_{\mathrm{AT}}}{2\cdot v_{\mathrm{orb}}}, \tag{2}$$

can be identified as the temporal lag between the interferometric pair. From (1) is is clear that larger baselines lead to better sensitivities. Too long baselines may result in a too small unambiguous velocity range (change of velocity that causes 2π rad ATI phase variation), and, usually before that, degradation of the phase quality due to temporal decorrelation of the radar echoes.

This baseline dependence of the ATI velocity estimate is illustrated in Fig. 1 for Low Earth Orbit (LEO) systems, where the cross-track surface velocity estimation error (σ_v) is shown as a function of the 1-way along-track baseline expressed in wavelengths for different wind velocities and SNR levels. A product resolution of 500×500 m^2 and 1×10^4 independent looks. Following [4], a Pierson-Moskowitz [5] spectrum is assumed so that the coherence time is given by

$$\tau_c = \frac{3\cdot\lambda}{U}\,\mathrm{erf}^{-1/2}\left(2.7\frac{\rho}{U^2}\right), \tag{3}$$

where U is the wind speed at the reference height, and ρ is the spatial resolution. Since there appears to be some common misunderstandings on how to interpret this spatial resolution, in particular for a SAR system observing the oceans, it is worth clarifying that for interferometric products the resolution of interest in (3) is the resolution of the final multi-looked product.

Qualitatively, it can be observed how the optimum baseline shifts towards smaller values for higher winds (larger ocean waves) and better SNRs. In practice, a compromise value needs to be found suitable for a range of sea state conditions. As a rule of thumb, 1-way ATI baselines around of 1000 - 2000 wavelengths appear to be a good choice. For example, at X-band this implies optimum physical baselines around 50 m.

It is clear that these order of optimum baselines can only be practically achieved using formation flying system concepts. Recent results have showcased the potential of such formation flying ATI acquisitions using TanDEM-X data [6, 7].

Ignoring again geophysical biases, ATI measurements are usually limited to measuring one component (at best) of the surface velocity vector. To overcome this limitation

Frasier and Camps [4] proposed a Dual Beam Interferometer (DBI) concept, where two interferometric pairs are formed with beams fore and aft squinted beams.

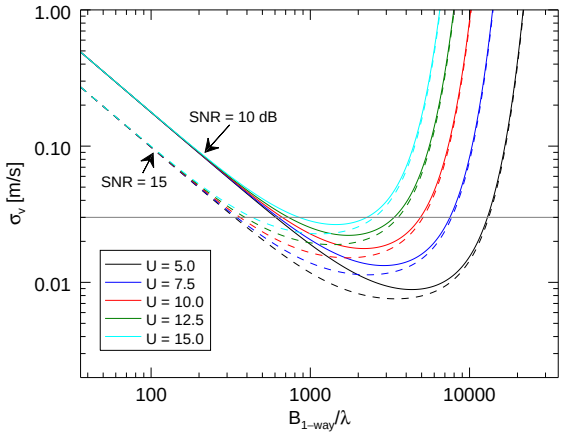

Figure 1: Standard deviation of cross-track surface velocity estimation error as a function of normalized 1-way baseline for different wind velocities, 25 degree incident angle, 500×500 m^2 product resolution with 10000 looks, and SNR levels of 10 and 15 dB

2 Bidirectional SAR ATI with TanDEM-X

The main objective of this paper is to explore the potential of combining this DBI concept with formation flying ATI. For this, we exploit the recently proposed Bidirectional (BiDI) SAR mode [8]. In this mode, the TerraSAR-X and TanDEM-X beams are squinted in azimuth to the maximum possible angle supported by the phased-array antenna, which is achieved by applying a linear phase tapering with a phase different between adjacent elements of π rad. Out of symmetry considerations it is easy to see that, with this tapering, the antenna produces a pair nominally symmetric beams squinted $\pm 2.2^\circ$ with respect to boresight (one can arbitrarily consider one of these beams as the main-lobe and the second as its dominant grating-lobe). The two beams imply a larger aggregated Doppler bandwidth, that needs to be accommodated by increasing the PRF. With the right choice of high PRF values, the two (strongly aliased) components can be separated in the Doppler frequency domain.

Although the beam separation is limited, it is sufficient to provide very good sensitivity to the along-track velocity components. This can be understood as inverting two orthogonal velocity components out of the projection of the velocity vector on two linearly independent (but far from orthogonal) vectors. For symmetric squints os $\pm\psi_\mathrm{s}$ (an assumption not made for the processing of the results shown later), an effective along-track velocity is estimated as

$$\tilde{v}_\mathrm{at} = \frac{\tilde{v}_\mathrm{r,fore} - \tilde{v}_\mathrm{r,aft}}{2 \sin \psi_\mathrm{s}}, \tag{4}$$

while the cross track (line-of-sight) velocity will be given by

$$\tilde{v}_\mathrm{r} = \frac{\tilde{v}_\mathrm{r,fore} + \tilde{v}_\mathrm{r,aft}}{2 \cos \psi_\mathrm{s}}. \tag{5}$$

Due to the different scalings, the LOS Doppler velocity uncertainty is a factor $\tan(\psi_\mathrm{s})$ smaller than the along-track one (a 0.04 factor in our particular geometry). However, if we are interested in the sensitivity to horizontal motions, the LOS velocity needs to be scaled by an additional $1/\sin\theta_\mathrm{i}$ term, so that the ratio of estimation uncertainties reduces to

$$\frac{\delta v_\mathrm{xt}}{\delta v_\mathrm{at}} = \frac{\tan \psi_\mathrm{s}}{\sin \theta_\mathrm{i}}. \tag{6}$$

It is interesting to consider the effect of the expected geophysical biases on the estimated along-track velocity. First, it is important to be aware that the fore and aft beams will receive echoes corresponding to different scattering centers. For a given patch of ocean surface, there will be a Doppler velocity bias that will be a function of the azimuth look direction (ϕ_a) with respect to some dominant wave direction (ϕ_0), incident angle, and the sea state,

$$\Delta v_\mathrm{r} = \mathrm{MTF}(\phi_\mathrm{a} - \phi_0, \theta_\mathrm{i}, \mathrm{sea\,state}). \tag{7}$$

For small squint angles, we can rewrite (4) as

$$\begin{aligned} \tilde{v}_\mathrm{at} &\approx \left.\frac{\partial \tilde{v}_r}{\partial \psi_\mathrm{s}}\right|_{\psi_\mathrm{s}=0} \\ &= \left.\frac{\partial \tilde{v}_r}{\partial \phi_\mathrm{a}} \cdot \frac{d\phi_\mathrm{a}}{d\psi_\mathrm{s}}\right|_{\phi_\mathrm{a}=0} = \frac{1}{\sin\theta_\mathrm{i}} \cdot \left.\frac{\partial \tilde{v}_r}{\partial \phi_\mathrm{a}}\right|_{\phi_\mathrm{a}=0}. \end{aligned} \tag{8}$$

Therefore, a simple $\cos(\phi_\mathrm{a} - \phi_0)$ azimuth angle dependence in (7) will lead to geophysical bias in the estimated along-track velocity off the form $\sin(\phi_0)$ with an extra $1/\sin(\theta_\mathrm{i})$ amplitude scaling.

3 Acquisitions

In total, 74 data-takes in BiDi bistatic TanDEM-X mode have been commanded for acquisition between the beginning of July 2013 and the beginning of November 2013 over five different test sites. These are located over ocean and sea ice scenes in the Northern Hemisphere between approximately 76 and 82 deg latitude including land for calibration purposes. The ascending and descending passes have been commanded in such a way that the orbits are crossing. The PRF lies in the range of approximately 5700 and 5900 Hz and the polarization is VV. The acquisition duration is about 40 s leading to an azimuth scene length of around 250 km. The mean along-track baseline varies between approximately 7 and 350 m and the mean effective baseline between 6 and 116 m. Continued acquisitions are already planned beyond the beginning of November 2013.

4 Experimental results

In this section we show results for a BiDI-ATI TanDEM-X acquisition made on September 13th, 2013. The scene is 210 km long and 26 km wide strip starting in the Kara Sea, South-East of the Northern tip of Novaya Zemlya, and ending North-West of it, in the Russian Arctic. Like in all BiDi-ATI acquisitions planned or acquired, land was included in the scene for calibration purposes. The physical along-track baseline between the two spacecraft increased from 53 m to 73 m during the acquisition, corresponding to ATI lags in the order of 4 ms. The formation geometry during the acquisition was such that the cross-track baseline was very small, yielding heights of ambiguity larger than 300 m, so that the XTI phase variations over the ocean surface are assumed to be negligible. A very steep incident angle, of approximately 16.7° was used, in part because the BiDi mode performs better at near range, where the high PRF required does not lead to high range ambiguities, but also due to the requirement of having land in the image.

Figure 2 shows the intensity, interferometric coherence, and the interferometric phase of the fore-beam. Due to the very steep incident angle, the NRCS of the ocean surface is higher than that of the partially ice-covered landmass. The short ATI baseline results in very high coherences over water. There is a degradation of the coherence in far-range resulting from a lower SNR due to the roll-off of the antenna pattern. The low SNR and low coherence feature at 130 km azimuth is most likely an intense raincell.

Since only a low precision Digital Elevation Model (DEM) of Novaya Zemlya was available, the interferometric phase has been flattened using the reference ellipsoid. The interferometric phases have been calibrated using as a reference all points over land with nominal heights in the range 2 m to 4 m have been used. The phase offset has been estimated by averaging the difference between the measured phased and the product of the nominal heights times the vertical wavenumber (k_z),

$$\Delta\phi = \frac{1}{N}\sum_i h_i \cdot k_{z,i}, \tag{9}$$

where k_z is given by $2\pi/h_{\mathrm{amb}}$. Note that k_z is slightly different for the fore and aft beams. Note that, due to the low quality of the reference DEM and some misalignment between the back-geocoded heights and the SAR images, there is surely some level of absolute phase uncertainty. However, remaining errors can be assumed to be common to the fore and the aft beams, so that they will introduce an offset in the line-of-sight observed Doppler velocities, but not on the estimated along-track velocities. In the figure, the interferometric phase has been clipped within a range off -1 rad to 1 rad in order to highlight phase variations over the ocean surface. On land, the phase variation of about two cycles is consistent with the topography of the island. Over water, ATI phase variations are clearly visible.

Figure 3 shows the estimated LOS Doppler velocity and *effective* along-track velocities at 250 x 250 m^2 resolution. We assume that most of estimated velocity is caused by wind-wave driven geophysical biases. Under this assumption, Fig. 4 shows the direction and relative strength of this bias, with the effective azimuth velocity multiplied by $\sin\theta_{\mathrm{i}}$ in order to compensate the scaling discussed at the end of Sec.2. In absence of ancillary data, a geophysical interpretation of these results is beyond the scope of this paper. Nevertheless, the overall picture seems geophysically consistent with wind-driven waves moving predominantly in the positive azimuth direction, which are discontinued on the left (North-West) side of Novaya Zemlya due to the lack of fetch.

5 Outlook

Future efforts will concentrate on systematically processing the large set off BiDi-ATI acquisitions already made, improving the interferometric calibration, and doing a geophysical analysis using ancillary information.

References

[1] R. M. Goldstein, H. A. Zebker, and T. P. Barnett, "Remote sensing of ocean currents," *Science*, vol. 246, no. 4935, pp. 1282–1285, Dec. 1989, PMID: 17832222.

[2] Bertrand Chapron, Fabrice Collard, and Fabrice Ardhuin, "Direct measurements of ocean surface velocity from space: Interpretation and validation," *Journal of Geophysical Research: Oceans*, vol. 110, no. C7, pp. n/a–n/a, 2005.

[3] R. Romeiser, H. Breit, M. Eineder, and H. Runge, "Demonstration of current measurements from space by along-track SAR interferometry with SRTM data," in *Geoscience and Remote Sensing Symposium, 2002. IGARSS '02. 2002 IEEE International*, 2002, vol. 1, pp. 158–160 vol.1.

[4] S.J. Frasier and A.J. Camps, "Dual-beam interferometry for ocean surface current vector mapping," *Geoscience and Remote Sensing, IEEE Transactions on*, vol. 39, no. 2, pp. 401–414, 2001.

[5] Willard J. Pierson Jr and Lionel Moskowitz, "A proposed spectral form for fully developed wind seas based on the similarity theory of s. a. kitaigorodskii," *Journal of Geophysical Research*, vol. 69, no. 24, pp. PP. 5181–5190, 1964.

[6] S. Suchandt and H. Runge, "First results of TanDEM-X along-track interferometry," in *Geoscience and Remote Sensing Symposium (IGARSS), 2012 IEEE International*, 2012, pp. 1908–1911.

[7] R. Romeiser, H. Runge, S. Suchandt, R. Kahle, C. Rossi, and P.S. Bell, "Quality assessment of surface current fields from TerraSAR-X and TanDEM-X along-track interferometry and doppler centroid analysis," *IEEE Transactions on Geoscience and Remote Sensing*, vol. Early Access Online, 2013.

[8] J. Mittermayer, S. Wollstadt, P. Prats-Iraola, P. Lopez-Dekker, G. Krieger, and A. Moreira, "Bidirectional SAR imaging mode," *IEEE Transactions on Geoscience and Remote Sensing*, vol. 51, no. 1, pp. 601 –614, Jan. 2013.

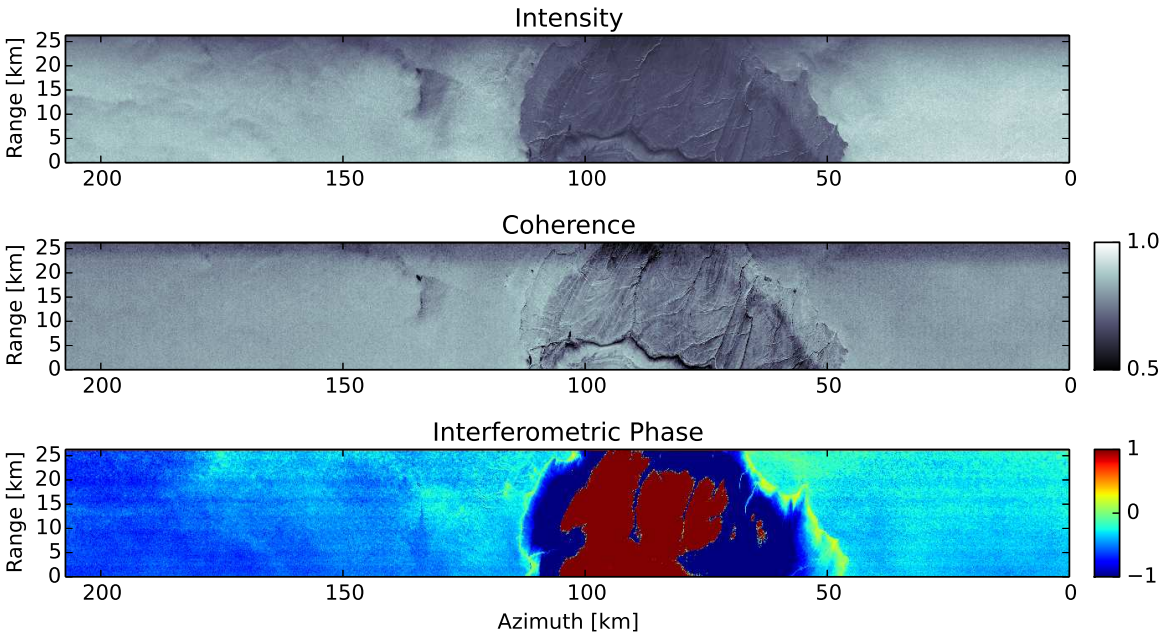

Figure 2: Intensity, interferometric coherence, and interferometric phase of fore-beam. Azimuth increases from right to left, with ground-range increasing from bottom to top, in accordance to the right-looking acquisition geometry of TanDEM-X. The land-mass visible in the azimuth interval 50 km to 121 km corresponds to the Northern tip of Novaya Zemlya, which divides the Russian Arctic and the Kara Sea.

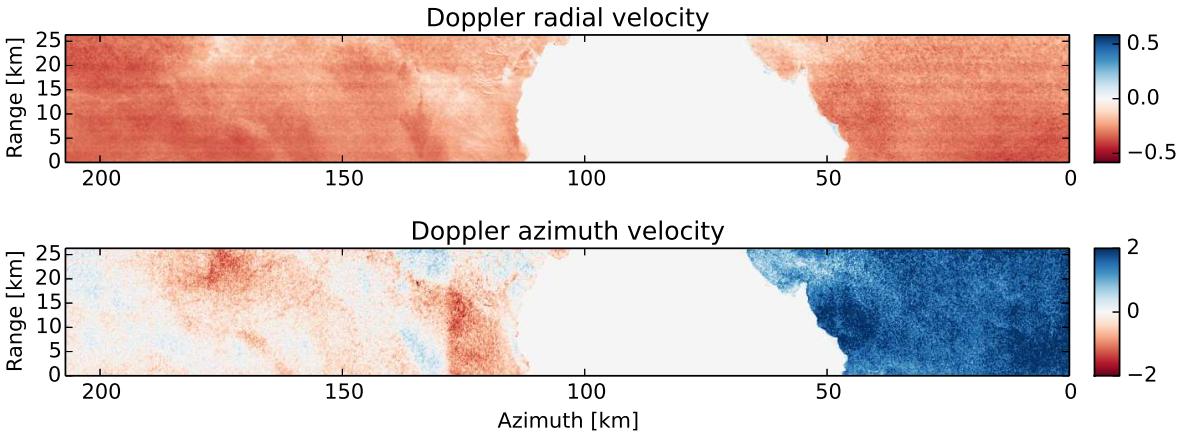

Figure 3: Estimated line-of-sight Doppler velocity (top) and estimated *equivalent* azimuth velocity (bottom). Positive LOS and azimuth velocities imply motions away from the radar and in the positive azimuth direction (right to left), respectively.

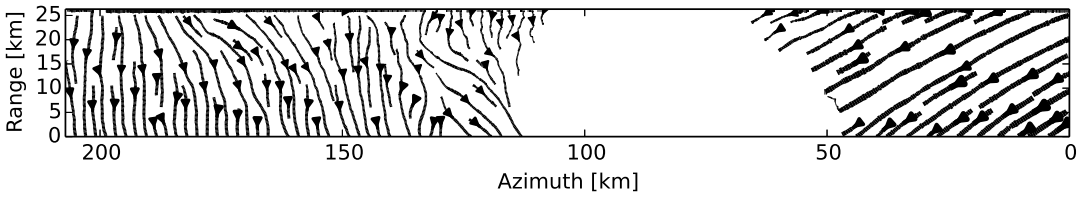

Figure 4: Effective 2-D Doppler velocity vector field.